Seismicity and Ground Motion Simulations of the SW Iberia Margin

M. Bezzeghoud, J.F. Borges, B. Caldeira

Geophysical Centre of Évora and Physics Department, ECT, University of Évora, Portugal

Abstract

In this study, we focus on the region between Gorringe Bank and the Horseshoe Fault located in the SW Iberia margin, which is believed to be the site of the great 1755 earthquake. We model ground motions using an extended source located near the Horseshoe scarp to generate synthetic waveforms using a wave propagation code, based on the finite-difference method. We compare the simulated waveforms using a 3-D velocity model down to the Moho discontinuity with a simple 1-D layered model. The radiated wave field is very sensitive to the velocity model and a small number of source parameters; in particular, the rupture directivity. The rupture directivity (controlled by the rupture initiation location), the strike direction and the fault dimensions are critical to the azimuthal distribution of the maximum amplitude oscillations. We show that the use of a stratified 1-D model is inappropriate in SW Iberia, where sources are located in the oceanic domain and receivers in the continental domain. The crustal structure varies dramatically along the ray paths, with large-scale heterogeneities of low or high velocities. Moreover, combined with the geometric limitations inherent to the region, a strong trade-off between several parameters is often observed; this is particularly critical when studying moderate magnitude earthquakes (M< 6), which constitute the bulk of the seismic catalogue in SW Iberia.

1. Introduction

The interaction between Iberia and Nubia results in a complex region located in the western part of the Eurasia–Nubia plate boundary (Fig. 1). This region corresponds to the transition from an oceanic boundary (between the Azores and the Gorringe Bank) to a continental boundary, where Iberia and Nubia meet (Borges et al., 2001; Buforn et al., 2004, Grandin et al., 2007a). The current tectonic regime at the boundary of the Nubian and Eurasian plates varies with longitude (Fig. 1) as a result of the rotation of Nubia, with respect to Eurasia, around a Euler pole located offshore Morocco, close to 20ºN, 20ºW (Argus et al., 1989; DeMets et al., 1994). This boundary can be divided into five sections (Bezzeghoud et al., 2008). To the west, between the
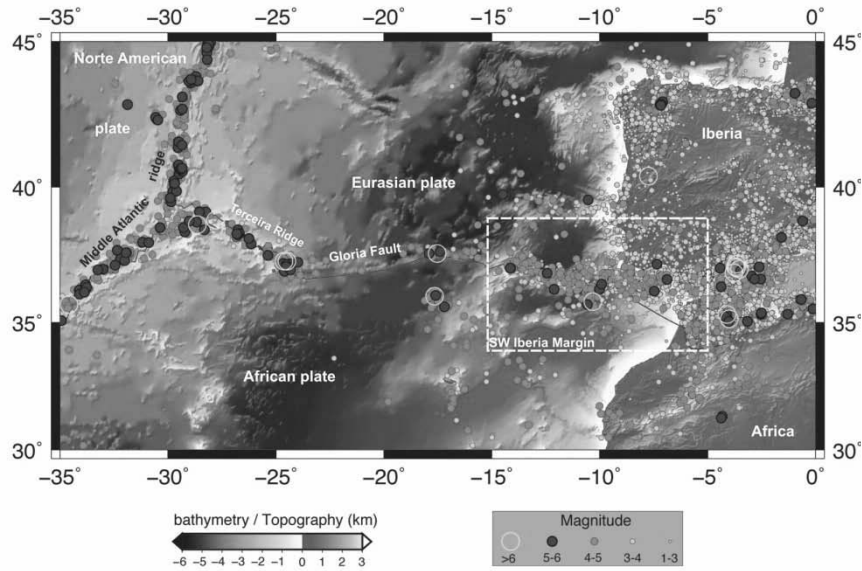
Fig. 1. Seismicity in the western part of the Eurasia–Nubia plate boundary
for the period 1973–2010 (NEIC Data File).

Nubia–Eurasia–North America triple junction (35ºW) on the eastern end
of the Terceira Ridge (24ºN), the regime is transtensional, with an extension
rate of 4.2 mm yr–1 (Borges et al., 2007, Borges et al., 2008; Bezzeghoud et
al., 2008), and is responsible for the active volcanism found in the Azores ar-
chipelago. In the central section, the relative motion of the two plates seems
to be accommodated by a single right-lateral fault, the Gloria Fault, although
significant seismic activity is observed in a broad region off the fault (Lynnes
& Ruff, 1985). East of 16ºW, the bathymetric continuation of the Gloria
Fault cannot be followed, and the definition of the boundary is less clear. A
transpressive tectonic regime dominates, with a very low convergence rate of
4 mm yr–1 (Argus et al., 1989; McClusky et al., 2003) trending NW-NNW,
consistent with the observed maximum horizontal stress direction (Ribeiro et
al., 1996; Borges et al,. 2001; Stich et al., 2003; Carrilho et al., 2004). Defor-
mation is distributed over an increasingly large area that reaches a N-S width
of 300 km near the continental margin of Iberia (Chen & Grimison, 1989). In
this section, the seismicity is scattered, with most events concentrated along a
100-km-wide band that trends ESE-WNW from 16ºW to 7ºW (Fig. 2). A
progressive shift of focal mechanisms, from strike-slip mechanisms in the
west to predominant reverse faulting in the east, has also been reported (Bu-

forn et al., 1988; Borges et al., 2001; Buforn et al., 2004) and can be interpreted as an increasing plunge of the minimum compression axis. In the Gulf
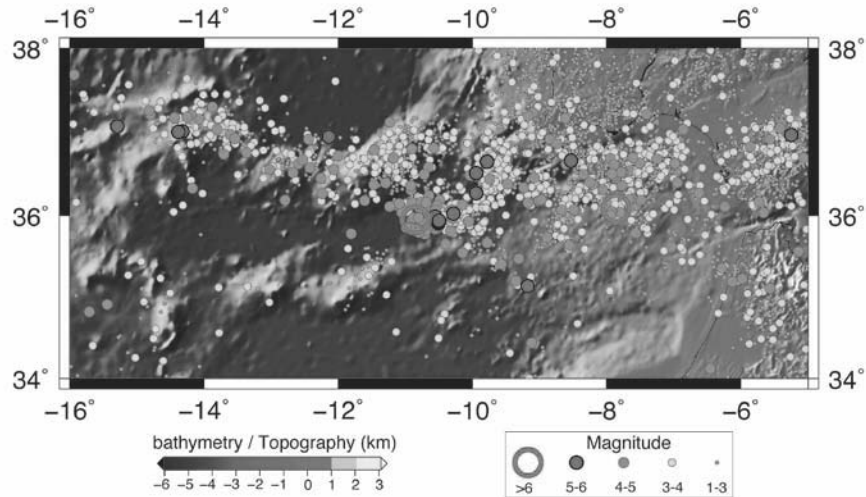

Fig. 2. - Seismicity provided by the Institute of Meteorology (IM, Portugal) in the southwestern Iberian margin for the period 1961–2010.

of Cadiz, the seismicity is denser to the north, around the Guadalquivir Bank (Fig. 2). East of the Strait of Gibraltar, in the Alboran domain and the Betic-Rif Arc, seismicity (Calvert et al., 2000) and GPS data (Fadil et al., 2006) both suggest that active deformation is spread over several hundred kilometres. In this study, we focus on the central section, which is believed to be the site of the great 1755 earthquake. We concentrate our analysis on ground motion modelling using an extended source located near the Horseshoe structure to generate synthetic waveforms using a wave propagation code based on the finite-difference method. We compare simulated waveforms using a 3-D velocity model down to the Moho discontinuity with a simple 1-D layered model. We confirm that the radiated wave field is very sensitive to the velocity model and the rupture directivity. The rupture directivity, strike direction and fault dimensions are critical factors for correctly modelling the azimuthal distribution of maximum amplitude oscillations.

2. Seismo-tectonic setting

The region east of 16°W is dominated by a transpressive tectonic regime, with a very low convergence rate between 4.0 and 5.5 mm/year (Argus et al., 1989; Buforn et al., 2004; Bezzeghoud et al., 2008) trending NW to NNW,

consistent with the observed maximum horizontal stress direction (Ribeiro et al., 1996; Borges et al., 2001; Jimenez-Munt et al., 2001). Deformation may be distributed over a large area (Chen and Grimison, 1988) as a result of the complex boundary conditions imposed on the Iberian plate (Andeweg et al., 1999; Jimenez-Munt et al., 2001). As a result of the complex tectonic history of the area, the western Iberian margin and its onshore extension are made up of a succession of uplifted blocks and areas of relative subsidence (Alves et al., 2003). East of 16°W, the absence of a continuous bathymetric trace along the Africa–Iberia boundary does not allow plate boundaries to be defined with certainty. An ongoing transition between passive and active margin stages of the Wilson cycle can explain the seismo-tectonic setting observed offshore (Ribeiro, 2002). In this region, we do not see a clear delineation between plates, and deformation is distributed over an increasingly large area that can reach a N-S width of 300 km near the continental margin of Iberia. The seismicity is scattered, but most events are concentrated along a 100-km-wide band, trending ESE-WNW from 16°W to 9°W. In this area, a series of topographic structures trend WSW-ENE (Zittelini et al., 2009). The Horseshoe scarp and the Marquês de Pombal scarp (Fig. 3), parallel to the St. Vicente Canyon, have experienced deformation since at least the Miocene. This scenario is supported by the occurrence of unusually large oceanic earthquakes within the area of scattered seismicity, such as the 1969 earthquake (Ms=8.0) and the 1755 Lisbon earthquake (Fig. 3, Table 1).
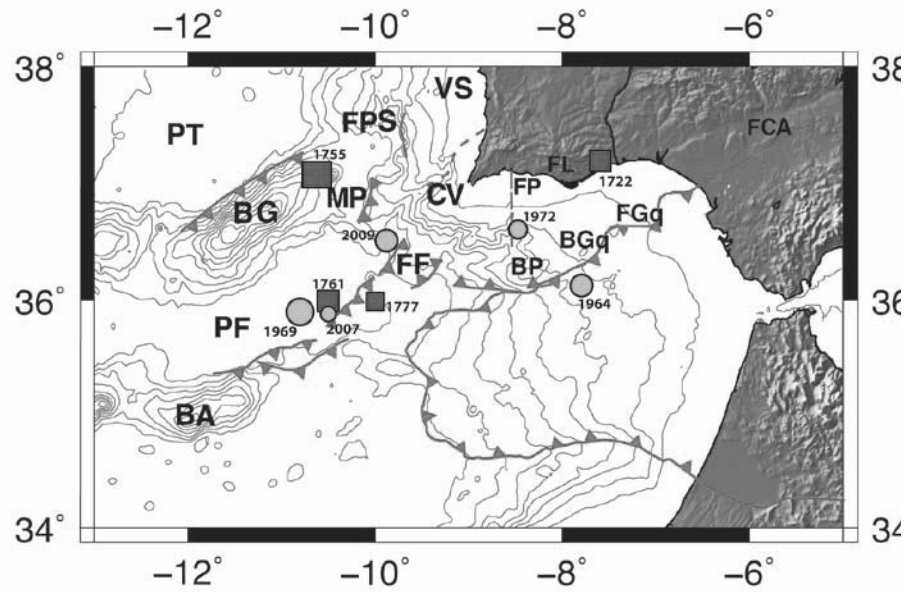
Fig. 3. - Significant earthquakes (see Table 1) and major active faults (adapted from Zitellini et al., 2009) in the southwestern Iberian margin. PT = Tejo plain; FPS: Pereira de Sousa Fault; PF = Horseshoe plain; FF= Horseshoe Fault; BA = Ampere bank; BGq = Guadalquivir bank; VS = Vale do Sado; MP = Marquês de Pombal Fault; BG = Gorringe bank; FGq = Guadalquivir Fault; FM = Messejana Fault; FL = Loulé Fault; FP = Portimão Fault; CV = St. Vicente Cape; FCA = Cadiz-Alicante Fault.

Table 1. Significant earthquakes in the southwestern part of the Iberian margin. Earthquakes from historical times to 1960 are taken from Sousa et al. (1992).

Date dd/mm/year	Lat.	Long.	Mw	Location
27/12/1722	37.2N	7.6W	7.5	Tavira (Algarve)
01/11/1755	37.0N	10.5W	8.5	SW S. Vicente Cape
31/03/1761	36.0N	10.5W	7.5	SW S. Vicente Cape
12/04/1777	36.0N	10.0W	7.0	SW S. Vicente Cape
15/03/1964	36.1N	7.8W	6.2	SE S. Vicente Cape
28/02/1969	35.9N	10.8W	7.5	SW S. Vicente Cape
12/02/2007	35.9N	10.5W	5.9	SW S. Vicente Cape
14/06/1972	36.6N	8.5W	5.2	SE S. Vicente Cape
17/12/2009	36.5N	9.9W	6.0	SW S. Vicente Cape

2.1. Instrumental seismicity

Onland, the seismicity exhibits significant scattering, with a maximum focal depth of 15–20 km (Buforn et al., 2004). In the Lusitanian basin, microseismicity reveals a complex pattern of focal mechanisms, and the depths of earthquakes, between 14 and 23 km, suggest that the sediment deformation is controlled by tectonic activity deep within the basement (Fonseca and Long, 1989). Seismic activity in the region of Évora is associated structures at un known depths (Borges et al., 2000). It is clearly possible to define microtremor alignments around Monchique that suggest a correlation with two probable faults that were recently identified in this area (Rocha et al., 2008; Rocha, 2010). In the NW region of Almodôvar, a trend in the distribution of epicentres may indicate the existence of an uncharted fault in this zone (Rocha, 2010).

In the last five years, there has been an increase in seismic activity in the area between Gorringe Bank and the Horseshoe Fault (Fig. 2). The largest recorded earthquake occurred offshore in 1969 (Mw=7.3), but since then, only two earthquakes have reached a magnitude of 6 (Table 1). These earthquakes all struck the region located between the Horseshoe Abyssal Plain and Cape St. Vicente where seismic activity decreases towards the coast. In this area, a series of topographic structures trending WSW-ENE exhibits clear seismic activity (Fig. 3). The Horseshoe scarp and the Marques de Pombal scarp, parallel to the St. Vicente Canyon (Fig. 3), show active deformation since at least the Miocene (Gràcia et al., 2003a) and are located above the transitional do-

main of the ocean–continent transition (OCT). The most prominent sea-mount is Gorringe Bank (Fig. 3), an uplifted thrust block of crustal and upper mantle rocks that culminates 25 m below sea level and was emplaced during the Miocene (12 Ma) by plate breakup, differential loading and NW-SE shortening of the Jurassic oceanic lithosphere (150 Ma) (Hayward et al., 1999). North of the Coral Patch Seamount and Coral Patch Ridge, scarps with the same trend affect the seafloor, and large amplitude folds involve the sedimentary cover down to the basement (Hayward et al., 1999). Most earth-quakes occurring in this zone (Figs. 2 and 3) are located at depths between 5 and 25 km and can reach 90 km (Buforn et al., 1988), even in the oceanic domain, where the Moho lies at a depth of 15 km. Despite large errors in hy-pocentral depth calculations (up to 10 km) due to poor azimuthal coverage, this suggests that brittle deformation also involves the upper mantle. The pas-sive western Iberian margin may be undergoing activation, with an incipient east-dipping subduction developing between the continental and transitional domains of the OCT, which might account for these observations (Ribeiro, 2002). Eastwards, widespread seismicity, with compressional and strike-slip fault plane solutions and a large, elongated positive free-air gravity anomaly, suggests that the Guadalquivir Bank is bounded by active faults (Grácia et al., 2003b). In the Guadalquivir foreland basin, seismicity is low (Figs. 2 and 3) and seems to be limited to the buried Subbetics frontal thrust.

2.2. Historical seismicity along the margin

Most major submarine canyons are aligned with NE-SW-trending faults on land, suggesting tectonic control over a broad area (Fig. 3). These faults were reactivated as reverse faults during Miocene compression, and historical re-cords of large earthquakes show that they are still active today (Fig. 3). The Nazaré Canyon corresponds to the Nazaré Fault, which has been active since the middle Cretaceous. It may be responsible for earthquake activity in the Batalha-Alcobaça region, with the latest event dating to 1890 (M=4.5). The Lower Tagus Fault Zone, whose seismo-tectonic interpretation is still under debate, might be extended by the Lisbon Canyon. This fault zone was active in 1344 (M=6.0), 1531 (M=7.1) and 1909 (M=6.0) (Moreira, 1982; Teves-Costa et al., 1999). The system may also have been activated during the 1755 Lisbon earthquake (Vilanova et al., 2003), suggesting a recurrence interval of 200 years. The source of the 1858 Setùbal earthquake (M=7.1) may be a blind thrust fault, trending NNE-SSW, located below the Setùbal Canyon, in the Sado Valley (Ribeiro, 2002). The St. Vicente Canyon is aligned with the Messejana Fault, a deep fault of lithospheric dimensions, showing 1 to 2 km of vertical throw in the upper crust on seismic profiles (Matias, 1996), but no

clear seismic activity. The Portimão Fault, dating to the Permian, shows seismic activity and can be followed along the Portimão Canyon. The Loulé Fault may accommodate a significant part of the shortening across the Algarve basin, due to the presence of halokinetic structures in its footwall, and may have exhibited recent seismic activity in 1587 (M=5.5) and 1856 (M=5.5) (Moreira, 1984; Terrinha, 1998). The source of the tsunamigenic 1722 Tavira earthquake (M=7.8) may be located offshore the southern Portuguese coast, possibly near the Guadalquivir bank area. The 1761 earthquake (M=8.0) also occurred offshore, generating a large tsunami, but its location is extremely uncertain (Baptista et al., 2006). This is also the case for the largest earthquake ever reported in Europe, which occurred in this region in 1755 (M=8.5), accompanied by a massive tsunami. For this event, different seismogenic origins are currently supported by various authors (e.g., Zitellini et al., 2001; Gutscher et al., 2002; Grandin et al., 2007b).

3. Ground motion modelling and directivity effects

3.1 – A 3-D velocity model and the 1755 earthquake source

A realistic velocity model, embedded in a wave propagation code, is an appropriate way to study the source parameters of the 1755 earthquake, provided that there are sufficient data. The finite-difference method is well adapted to this strategy, because it has sufficient computational efficiency to enable a large number of tests and is accurate in the low-frequency range (f < 0.5 Hz), which is most significant for studying the destructive effects of large earthquakes at the regional scale. The velocity model used here was proposed and validated by Grandin et al. (2007a).

The velocity model of the crust used in this study incorporates the major seismogenic centres observed offshore SW Iberia, between Gorringe Bank and the Betic Cordillera in the region lying between latitudes 35.2ºN and 39.7ºN and between longitudes 11.8ºW and 6.1ºW. The crust is stratified and is made of a superposition of a finite number of layers, with varying depths and thicknesses. Only the depth of each interface between layers must be specified at given points; then, a Delaunay triangulation can be applied to fill the spaces between these points (Watson, 1982). A layer can thus taper off and reach zero thickness, if necessary, which is convenient for modelling sedimentary basins or the OCT: To account for their complex geometries and high variations of thickness/depth, these regions only require a denser network of data points. We also assumed that both continental and oceanic crust could be described with the same layers, by coupling layers that have similar

wave propagation velocities and densities in the two domains. The links between coupled layers are assessed based on seismic profiles. However, their resolutions are often insufficient to locate small lateral velocity discontinuities, and we thus focus on large wavelength variations of major intra-crustal layer thicknesses. In this model, the purely oceanic crust is separated from the continental crust by a transitional domain, probably made up of thinned, highly faulted or intruded continental crust. The classification for continental crust layers uses nine different layers with distinct physical identified properties. These overlie the upper mantle, which is modelled as a half-space, with a uniform velocity of 8.1 km/s and a Vp/Vs ratio of 1.74 to deduce S-wave velocities from P-wave velocities (Grandin et al., 2007a). Densities were set based on experimental measures of density for a set of crustal rocks. The complete SWIB2006 velocity model is discussed in Grandin et al. (2007a) and posted on the webpage:
http://evunix.uevora.pt/~jborges/3DSEISM/get_SWIBmod.html;   it   is freely available to the public.

The 1755 November 1 earthquake was the strongest earthquake ever reported in Europe and was extremely destructive (Portugal: Pereira de Sousa 1919; Spain: Martínez-Solares et al., 1979; Morocco: Levret, 1991) – the shock was felt even in Northern Germany, the Azores and the Cape Verde Islands (Reid, 1914). The large size of the earthquake is further evidenced by observations of seiches in southern England and Holland and as far as Finland (Reid, 1914). The large tsunami waves generated by the earthquake also caused extensive damage along the coasts of Portugal, southern Spain and Morocco and were even detected in the Lesser Antilles and southwestern England. Extensive geological evidence of tsunami deposits associated with the 1755 earthquake has been reported in Europe (e.g., Andrade, 1992; Dawson et al., 1995; Abrantes et al., 2005; Scheffers & Kelletat, 2005). The problem of epicentral location has been addressed by various early studies (Reid, 1914; Pereira de Sousa, 1919), and since the beginning of the instrumental period, a consensus has attributed the origin of the earthquake to a structure located between the Gorringe Bank and the Coral Patch Ridge (Machado, 1966; Moreira, 1985; Johnston, 1996; Grandin et al., 2007b). In the most recent hypothesis, Grandin et al. (2007b) tested, by forward modelling, three published sources for the 1755 earthquake that can be considered as end-members of the set of proposed offshore seismic sources (Johnston, 1996; Zitellini et al., 2001; Terrinha et al., 2003; Gutscher et al., 2002; Gutscher et al., 2006; Thiebot & Gutscher, 2006). Following the results of these tests, Grandin et al. (2007b) concluded that a fault located below Gorringe Bank, with a rupture directed towards the SW, reproduces the overall pattern of macroseismic observations better than a fault aligned along the Marquês de Pombal–Pereira de Sousa Fault zone or a subduction-related thrust fault in the Gulf of Cádiz. Except for Grandin et al. (2007b), all seismic modelling of the 1755 Lisbon

earthquake performed by various authors (Mendes-Victor et al., 1999; Baptista et al., 2003; Gutscher et al., 2006) suffer limitations, because they do not take into account physical considerations related to the complexity and directivity of the seismic source on one hand, or the propagation medium on the other hand (Grandin et al., 2007a,b).

3.2 - Propagation medium and directivity of the seismic source

To model the propagation of seismic waves in a 3-D medium, we used the code E3D, an explicit 2-D/3-D elastic finite-difference wave propagation code (Larsen & Schultz, 1995) based on the work of Madariaga (1976). The method, computational issues related to the finite-difference scheme and source implementation are given in detail in Grandin et al. (2007a,b). The method has been successfully applied by a large number of authors to generate synthetic seismograms (e.g., Olsen & Archuleta, 1996; Larsen et al., 1997; Dreger et al., 2001; Pitarka et al., 2004; Hartzell et al., 2006; Kagawa et al., 2004; Grandin et al., 2007a,b).

For a source like that of the 1755 Lisbon earthquake (Mw~8.5), the finiteness of the fault dimensions and of the duration of rupture cannot be ignored. Following the source implementation scheme of E3D, we model this extended source by superimposing a large number of point sources over a rectangular fault plane that has the same strike and dip as the individual subevents. The kinematics of the rupture, namely, the rupture propagation direction, are simulated by triggering a rupture on each subfault at the right time: a rupture can nucleate at a certain location on the fault and then propagate radially until the fault edge is reached – the rupture velocity is assumed to be constant over the fault plane. To prevent high-frequency noise from entering the radiated spectrum and to thus generate a smooth source time function, it is important that the rupture on each subfault is initiated before the rupture on the previous adjacent subfault has stopped. We chose to use a Brune signal as the elementary source time function for rupture on each subfault (Brune, 1970). In the case of a finite source, the rupture velocity is fixed at 2.5 km s–1 and the grid spacing is 1 km (maximum frequency of 0.3 Hz). We also assume a uniform seismic moment distribution over the fault plane. Thus, the slip is not uniform, due to variations in the rigidity modulus with depth in the velocity model. However, in the epicentral distance range considered here (d > 100 km), we have verified that this condition does not induce significant differences from a uniform geometric moment distribution. Furthermore, we set the depth to the top of the fault so that co-seismic rupture does not extend beyond the seismic basement. This prevents the occurrence of super-shear rupture velocities in the shallow sedimentary cover, but

assumes that sediments are not involved in significant seismic wave generation. This hypothesis is valid from a seismological point of view (Grandin et al., 2007b).

The stability of this method has already been verified by Grandin et al. (2007a,b) through a large number of simulations to evaluate the importance of the arbitrarily fixed parameters, such as the characteristic time of subevent rupture, which sets both the rise time and the duration of the rupture, the rupture velocity, and the complex geometry. On the other hand, variations in the focal parameters, fault plane geometry and rupture directivity have strong effects on the resulting radiated wave field. The computational domain has a grid spacing of 1 km and extends to a depth of 70 km.

**Table 2.** - Source parameters used to compute synthetic waveforms.

Scenario	Nucleation point X; Y (km)	Fault area L x W	H km	M_o x 10^{22} (Nm)	M_w	Strike	Dip	Rake	Vr (km/s)
Directive	53.33; 50	200 x 80	8	1.16	8.7	60	40	90	2.7
Bi-directive	53.33; 0								
Anti directive	53.33; - 50								

For this study, we compare simulated waveforms based on the source parameters given in Table 2 for a 3-D velocity model down to the Moho discontinuity versus a simple 1-D layered model (Figs. 4 and 5). We confirm that the radiated wave field is very sensitive to the velocity model (Fig. 5) and a small number of source parameters; in particular, the rupture directivity (Fig. 6). In contrast, the computation is not very sensitive to other source parameters, such as the dip, the rake, the rupture velocity, the depth to the top of the fault or the duration and shape of the source time function. Figures 4 and 5 show that the use of a stratified 1-D model is definitively inappropriate in SW Iberia, where sources are located in the oceanic domain and receivers in the continental domain; the crustal structure varies dramatically along the ray
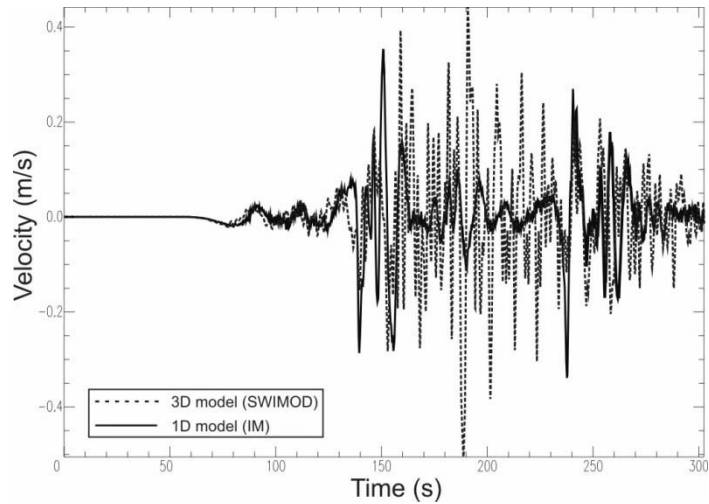
Fig. 4. - Comparison between simulated waveforms obtained using a 3-D velocity model and a simple 1-D layered model for the first point close to Faro city (see profile located on the top of the 3-D structure model of Fig. 5).

paths, with large-scale heterogeneities of low or high velocities. Figure 5 shows that in the Mesozoic basin, the 3-D velocity model gives maximum velocity values that are about a factor of two higher than those given by the 1-D velocity model. Moreover, combined with the geometric limitations inherent to the region, a strong trade-off between several parameters is often observed: this is particularly critical when studying moderate magnitude earthquakes (M< 6), which constitute the bulk of the seismic catalogue in SW Iberia. Figure 6 shows the significance of the directivity effect, which is controlled by the rupture initiation location, for three rupture scenarios: directive, anti-directive and bi-lateral. The directive rupture gives the maximum velocity values; in the Mesozoic basin, they are greater than those of the anti-directive rupture by a factor of about 6 and are greater than those of the bilateral rupture by a factor of 3.5. The rupture directivity, velocity model, strike direction and fault dimensions are critical factors controlling the azimuthal distribution of the maximum amplitude oscillations. The radiation that issues from an extended seismic source when a rupture spreads in preferential directions can be distinguished from that emitted by a point source. This distinctive characteristic, which is known as directivity (Ben-Menahem, 1961), is manifested by an increase in the frequency and amplitude of seismic waves when the ruptu-
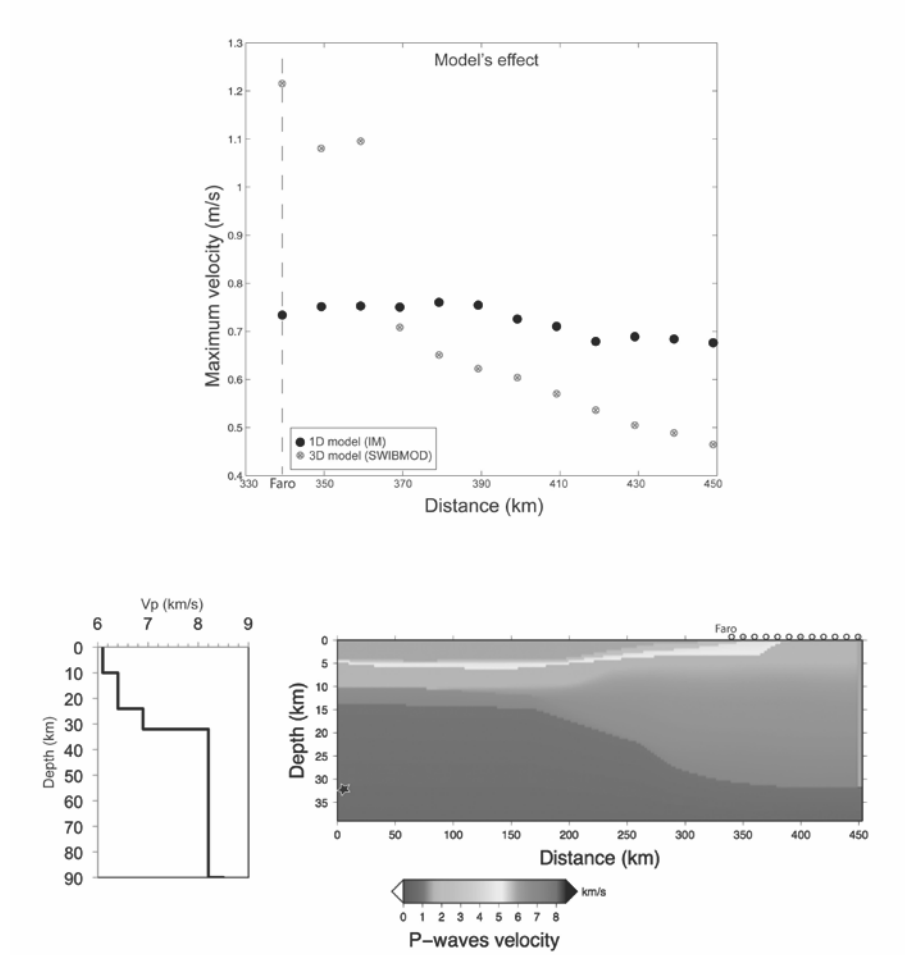
Fig. 5. - Top: 3-D velocity model effects. Comparison between simulated maximum velocities obtained using a 3-D velocity model with a simple 1-D layered model along the line, represented by open circles, shown on top of the 3-D P-wave velocity model represented below. Below: 1-D P-wave velocity model (left) and 3-D P-wave velocity model (right) extracted from the SWIBMOD (Grandin et al., 2007a), model along the profile located at the bottom of Fig. 6.

re occurs in the direction of the seismic station and a decrease if it occurs in the opposite direction (e.g., Caldeira et al., 2009). Moreover, these effects are not present when the rupture direction is perpendicular to the propagation direction.
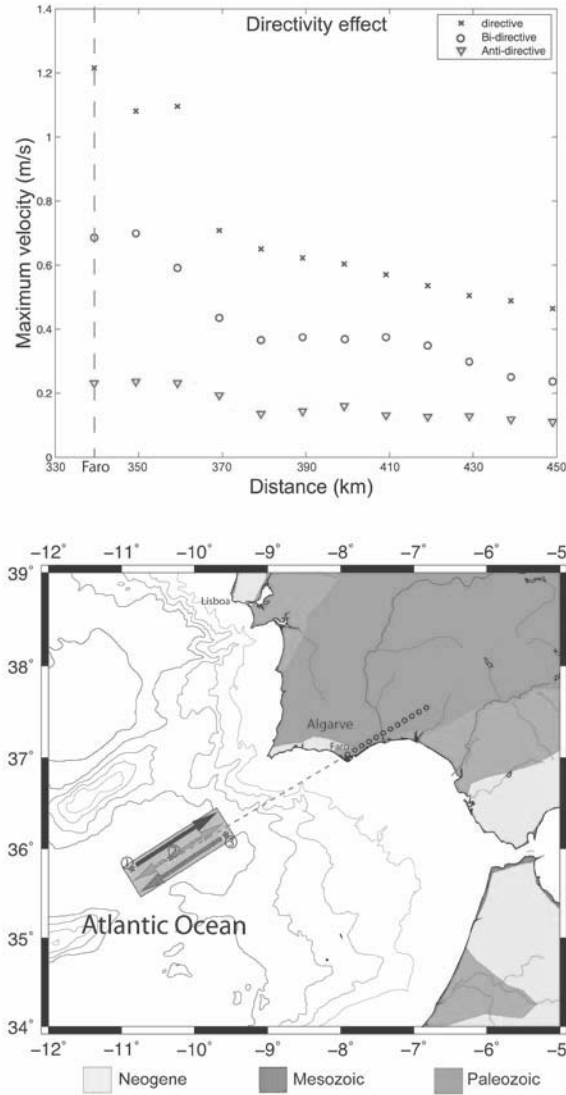
Fig. 6. - Top: Directivity effect. Comparison of simulated maximum velocities obtained using a 3-D velocity model for the 3 proposed rupture process scenarios: directive, bi-lateral and anti-directive. Bottom: Source location and rupture process used for the simulated waveforms determined in this study. Red star=the epicentre, arrows=average direction and the extent of the rupture front during the related period for the directive, bi-lateral and anti-directive scenarios. Open circles=the profile where simulated waveforms are determined. The corresponding values are indicated at the tops of Figs. 5, 6.

4. Discussion

Most great tsunamigenic earthquakes are related to well-defined interplate convergence zones: the circum-Pacific seismic belt, the Sunda arc, the Hellenic arc or the Antilles arc. One exception is the massive earthquake that struck Iberia and Morocco on November 1, 1755, which was felt throughout a large part of Europe and produced a powerful tsunami that crossed the Atlantic Ocean. This earthquake occurred along a passive margin, in a region where plate boundaries are not unequivocally defined by bathymetry and where the existence of an active subduction zone is not clearly supported by seismological evidence. Thus, despite the large size of the fault that was responsible for this extreme event (several hundred kilometres), many hypotheses have been proposed by various authors regarding its location (Grandin et al., 2007b). However, a fault located below Gorringe Bank, with a rupture directed towards the SW, better reproduces the overall pattern of macroseismic observations than a fault aligned along the Marquês de Pombal–Pereira de Sousa Fault zone or a subduction-related thrust fault in the Gulf of Cádiz (Grandin et al., 2007b).

Observations from the mega (Mw 9.3) earthquake of December 2004 in Sumatra and the Mw 8.8 Maule (Chile) earthquake offer new insights concerning rupture and tsunami generation in great subduction earthquakes, which may be applicable to the study of the 1755 earthquake and tsunami. The earthquake of 1755 generated a tsunami with waves about 6 m high at Lisbon, 15 m high along the coast of the Algarve and 20 m high at Cadiz, Spain. The waves travelled on to Martinique, a distance of 6100 km, in 10 hours and there rose to a height of 4 m. For the Sumatra mega earthquake, the waves may have been 15 to 30 m high along the entire 100-km stretch of coast from Kreung Sabe to the northwestern part of the island (USGS).

The great Lisbon earthquake of 1 November 1755 (Mw~9.0) probably released as much or more energy as any seismic event in recorded history prior to December 2004. The Azores–Gilbratar fracture zone (AGFZ) marks the boundary of active tectonic interaction between the African and Eurasian plates. This is an active seismic region where large earthquakes occur frequently, and some of them, near the eastern segment of the AGFZ, are capable of generating tsunamis. The tectonic interactions of the eastern segment of the AGFZ involve a thrusting component in the NW direction along a NE-trending strike plane (Buforn et al., 2004; Grandin et al., 2007b; Bezzeghoud et al., 2008).

An earthquake rupture can spread across a fault in a variety of ways. However, the fundamental characteristics of the rupture propagation are based mainly on the rupture directivity (unilateral or bilateral). Based on a study of large and moderate shallow earthquakes ($M \geq 7.0$),   McGuire et al. (2002)

showed that the majority of large earthquakes have a predominantly unilateral rupture. This observation quantifies what appears to be a general property of large earthquake dynamics. The unilateral character determined for the Mw 9.3 and 8.7 Sumatra earthquakes (Bezzeghoud et al., 2005), for the Mw 8.5 1755 Lisbon earthquake (Grandin et al., 2007b) and for the recent Mw 8.8 Maule (Chile) earthquake of 27 February 2008 (Raul Madariaga, personal communication) supports the observation made by McGuire et al. (2002) that ruptures are predominantly unilateral. Furthermore, numerous studies of extended-source earthquake models examining the spatial and temporal evolution of earthquake slip on fault planes have shown that slips are spatially variable, and 48% of events nucleate in regions of low slip (Mai et al., 2005). This behaviour was also observed for the 2004 and 2005 Sumatra earthquakes (Bezzeghoud et al., 2005).

The results of this study clearly show that earthquake directivity is the focusing of wave energy along the fault in the direction of rupture. This means that, exclusive of local site conditions such as soft soils, the stronger ground motions and damage (if the earthquake is large enough) will be distributed in an elongated pattern centred along the axis of the fault. The distance to the fault is not the only consideration for ground motion amplitude: the structure and the rupture directivity are also important. When a fault ruptures unilaterally (with the epicentre at or near one end of the fault break), the radiated waves are stronger in one direction along the fault. The characteristics of ground shaking close to a fault rupture generally depend on whether the rupture moves towards the building site or away from it. These two cases are often referred to as forward and backward directivity conditions, respectively. In the forward directivity case, the ground motion tends to have a pulse that is often very apparent in the velocity time histories. The average period of such pulses, which appears to depend on magnitude, may vary from about 1.5 s for a Mw 6.5 event to more than 3 s for a Mw 7.5 earthquake (Somerville, 2003). These moderate-to-long period pulses have been recognised to generate, on average, systematically larger responses in moderate-to-long period structures, as compared to the responses induced by more typical "rumbling" ground motions of similar severity. The latter ground motions are more common both at sites that are located close to the causative fault but in the backward directivity region and at sites that are far away from the rupture.

We conclude that it is very important, particularly in seismic risk studies, to take into account the rupture directivity and 3-D velocity model. This provides encouraging results for the computation of low-frequency seismograms in the region and can be used to study larger earthquakes, for which the radiated wave field has a predominant low-frequency spectrum

Acknowledgments

References

Andrade, C., 1992. Tsunami generated forms in the Algarve barrier islands (south Portugal), Sci. Tsunami Hazards, 10(1), 21–34.

Alves, T.M., Gawthorpe, R.L., Hunt,D.W.&Monteiro, J.H., 2003. Cenozoic tectonosedimentary evolution of theWestern Iberian Margin, Mar. Geol., 195, 75–108.

Andeweg B., G. De Vicente, S. Cloetingh, J. Giner, A. Muñoz Martin, 1999. Local stress fields and intraplate deformation of Iberia: variations in spatial and temporal interplay of regional stress sources. Tectonophysics 305, 153–164.

Argus, D.F., Gordon, R.G., DeMets, C. & Stein, S., 1989. Closure of the Africa-Eurasia-North America plate motion circuit and tectonics of the Gloria fault, J. geophys. Res., 94, 5585–5602.

Ben-Menahem A, 1961. Radiation of seismic surfacewaves from finite moving sources. Bull Seismol Soc Am 51:401–435

Baptista, M.A., Miranda, J.M. & Luis, J.F., 2006. In Search of the 31 March 1761 Earthquake and Tsunami Source, Bull. Seism. Soc. Am., 96(2), 713–721.

Bezzeghoud M., J. F. Borges, B. Caldeira, E. Buforn, A. Udias, 2008. Seismic activity in the Azores Region in the context of the western part of the Eurasia-Nubia plate boundary. International Seminar on Seismic risk and rehabilitation on the 10th Anniversary of the July 9 1998 Azores Earthquake, Horta-Azores, 9-13 July. 27-31.

ezzeghoud M., J.F. Borges & Caldeira B., 2005. The 2004 and 2005 Sumatra earthquakes. Implications for the Lisbon earthquake. 250th Anniversary of the 1755 Lisbon Earthquake. International Conference, 1-4 Nov. 2005, Lisbon, Portugal. 592-598

Borges, F. F., M. Bezzeghoud, B. Caldeira, E. Buforn, 2008, Recent Seismic Activity in the Azores Region. International Seminar on Seismic risk and rehabilitation on the 10th Anniversary of the July 9 1998 Azores Earthquake, Horta-Azores, 9-13 July. 33-37.

Borges, J.F., Fitas, A.J.S., Bezzeghoud, M., & Teves-Costa, P., 2001. Seismotectonics of Portugal and its adjacent Atlantic area, Tectonophysics, 337, 373–387.

Borges J. F., M. Bezzeghoud, E. Buforn, C. Pro & A. Fitas, 2007. The 1980, 1997 and 1998 Azores earthquakes and its seismotectonic implications. Tectonophysics, 435, 37-54.

Buforn, E., Udías, A. & Colombás, M.A.,1988a. Seismicity, source mechanisms and seismotectonics of the Azores-Gibraltar plate boundary. Tectonophysics, 152, 89-118.

Buforn, E., Bezzeghoud, M., Udías, A. & Pro, C., 2004. Seismic sources on the Iberia-African plate boundary and their tectonic implications, Pure Appl. Geophys., 161.

Carrilho, F., P. Teves-Costa, I. Morais, J. Pagarete & R. Dias, 2004. Geoalgar Project – first results on seismicity and fault-plane solutions. Pure and Applied Geophys., 161, 3, 589-606.

Caldeira, B., Bezzeghoud M., Borges J. F., 2009, DIRDOP: a directivity approach to determining the seismic rupture velocity vector, Journal of Seismology, in open access, DOI: 10.1007/s10950-009-9183-x.

Calvert, A. Sandvol, E. Seber, D., Barazangi, M., Roecker, S., Mourabit, T., Vidal, F. Alguacil, G. Jabour, N., 2000. Geodynamic evolution of the lithosphere and upper mantle beneath the Albor´an region of the western Mediterranean: constraints from travel time tomography, J. Geophys. Res., 105, 10 871–10 898.

Chen, W.P. & Grimison, N., 1989. Earthquakes associated with diffuse zones of deformation in the oceanic lithosphere: some examples, Tectonophysics, 166, 133–150.

Dawson, A.G., Hindson, R., Andrade, C., Freitas, C., Parish, R. & Bateman, M., 1995. Tsunami sedimentation associated with the Lisbon earthquake of 1 November AD 1755: Boca do Rio, Algarve, Portugal, The Holocene, 5(2), 209–215.

DeMets, C., R.G. Gordon, D.F. Argus, & D. Stein, 1994. Effect of recent revisions to the geomagnetic reversal time scale and estimates of current plate motions, Geophys. Res. Lett., 21, 2191-2194.

Fadil, A., Vernant, P., McClusky, S., Reilinger, R., Gomez, F., Ben Sari, D., Mourabit, T., Feigl, K. & Barazangi, M., 2006. Active tectonics of the western Mediterranean: Geodetic evidence for rollback of a delaminated subcontinental lithospheric slab beneath the Rif Mountains, Morocco, Geology, 34(7), 529–532.

Fonseca, J.F.B.D. & Long, R.E., 1991. Seismotectonics of SW Iberia: a distributed plate margin? in Seismicity, Seismotectonics, and Seismic Risk of the Ibero-Maghrebian Region, eds Mezcua, J. & Udías, A., Memoir 8, Instituto Geografico Nacional, Madrid.

Grácia, E., Dañobeitia, J., Vergés, J., 2003a. Mapping active faults offshore Portugal (36ºN–38ºN): implications for the seismic hazard assessment along the southwest Iberian margin, Geology, 31(1), 83–86.

Grácia, E., Dañobeitia, J., Vergés, J., Bartolomé, R. & Córdoba, D., 2003b. Crustal architecture and tectonic evolution of the Gulf of Cadiz (SW Iberian margin) at the convergence of the Eurasian and African plates, Tectonics, 22(4).

Grandin R., Borges J.F., Bezzeghoud M., Caldeira B., Carrilho F., 2007a. Simulations of strong ground motion in SW Iberia for the 1969 February 28 (MS = 8.0) and the 1755 November 1 (M ~ 8.5) earthquakes – I. Velocity model, Geophys. J. Int., Vol. 171, Issue 3, 1144–1161.

Grandin R., Borges J.F., Bezzeghoud M., Caldeira B., Carrilho F., 2007b. Simulations of strong ground motion in SW Iberia for the 1969 February 28 (MS = 8.0) and the 1755 November 1 (M ~ 8.5) earthquakes – II. Strong ground motion simulations, Geophys. J. Int., Vol. 171, Issue 2, 807-822, November 2007.

Gutscher, M.A., Malod, J., Rehault, J.P., Contrucci, I., Klingelhoefer, F., Mendes-Victor, L.&Spackman,W., 2002. Evidence for active subduction beneath Gibraltar, Geology, 30, 1071–1074.

Gutscher, M.-A., Baptista, M.A., Miranda, J.M., 2006. The Gibraltar Arc seismogenic zone. Part 2: constraints on a shallow east dipping fault plane source for the 1755 Lisbon earthquake provided by ts Baptista et al., 2003 unami modeling and seismic intensity, Tectonophysics, 426(1–2), 153–166.

Hartzell, S. et al., 2006. Modeling and Validation of a 3D Velocity Structure for the Santa Clara Valley, California, for Seismic-Wave Simulations, Bull. Seism. Soc. Am., 96(5), 1851–1881.

Hayward, N., Watts, A.B., Westbrook, G.K. & Collier, J.S., 1999. A seismic reflection and GLORIA study of compressional deformation in the Gorringe Bank region, eastern North Atlantic, Geophys. J. Int., 138, 831–

850.

Jiménez-Munt, I., Fernàndez, M., Torne, M. & Bird, P., 2001. The transition from linear to diffuse plate boundary in the Azores-Gibraltar region: results from a thin-sheet model, Earth. Planet. Sci. Lett., 192, 175–189.

Johnston, A., 1996. Seismic moment assessment of earthquakes in stable continental regions – III. New Madrid 1811–1812, Charleston 1886 and Lisbon 1755, Geophys. J. Int., 126, 314–344.

Kagawa, T., Zhao, B., Miyakoshi, K. & Irikura, K., 2004. Modeling of 3D basin structures for seismic wave simulations based on available information on the target area: case study of the Osaka Basin, Japan, Bull. Seism. Soc. Am., 94, 1353–1368.

Larsen, S.C. & Schultz, C.A., 1995. ELAS3D, 2D/3D Elastic Finite- Difference Wave Propagation Code, Lawrence Livermore National Laboratory, UCRLMA-121792, 18 pp.

Larsen, S., Antolik, M., Dreger, D., Stidham, C., Schultz, C., Lomax, A. & Romanowicz, B., 1997. 3D models of seismic wave propagation; simulating scenario earthquakes along the Hayward Fault, Seism. Res. Lett., 68(2), 328.

Levret, A., 1991. The effects of the November 1st, 1755 "Lisbon" earthquake in Morocco, Tectonophysics, 193, 83–94.

Lynnes, C.S. & Ruff, L.J., 1985. Source process and tectonic implications of the great 1975 North Atlantic earthquake, Geophys. J. R. astr. Soc., 82, 497–510.

Madariaga, R., 1976. Dynamics of an expanding circular fault, Bull. Seism. Soc. Am., 66(3), 639–666.

Matias, L.M., 1996. A sismologia experimental na modelaç̃ao da estrutura da crusta em Portugal continental, Ph.D. thesis. Univ. of Lisbon, 398 pp.

McGuire, J. J., L. Zhao, & T. H. Jordan, 2002. Predominance of unilateral rupture for a global catalog of earthquakes, Bull. Seismol. Soc. Am. , 92 , 3309-3317.

McClusky, S., Reilinger, R., Mahmoud, S., Ben Sari, D. & Tealeb, A., 2003. GPS constraints on Africa (Nubia) and Arabia plate motions, Geophys. J. Int., 155, 126–138.

Mendes-Victor, L., Baptista, M.A., Miranda, J.M. & Miranda, P.M.A., 1999. Can hydrodynamic modelling of tsunami contribute to seismic risk assessment? Phys. Chem. Earth, 24, 139–144.

Martínez-Solares, J.M., Lopez, A. & Mezcua, J., 1979. Isoseismal map of the 1755 Lisbon earthquake obtained from Spanish data, Tectonophysics, 53, 301–313.

Machado, F., 1966. Contribuição para o estudo do terremoto do terramoto de 1 de Novembro de 1755, Rev. Fac. Ciências, Lisboa, C14, 19–31.

Moreira VS, 1982. Sismotectónica de Portugal Continental e Região Atlântica adjacente. INMG, Lisboa. (In Portuguese)

Moreira, V.S., 1984. Sismicidade histórica de Portugal Continental, Revista do Instituto Nacional de Meteorologia e Geofísica, Lisbon, pp. 79. (In Portuguese)

Moreira, V.S., 1985. Seismotectonics of Portugal and its adjacent area in the Atlantic, Tectonophysics, 11, 85–96.

Olsen, K.B. & Archuleta, R.J., 1996. Site response in the Los Angeles Basin from 3-D simulations of ground motion, SRL, 67(2), p. 49.

Pereira de Sousa, F.L., 1919. O terremoto do 1º de Novembro de 1755 em Portugal e um estudo demográfico (Serviços Geológicos de Portugal), Vol. I-IV. (In Portuguese)

Pitarka, A., Graves, R. & Sommerville, P., 2004. Validation of a 3D velocity model of the Puget Sound region based on modeling ground motion from the 28 February 2001 Nisqually earthquake, Bull. Seism. Soc. Am., 94(5), 1670–1689.

Ribeiro, A., Cabral, J., Baptista, R., Matias, L., 1996. Stress pattern in Portugal mainland and the adjacent Atlantic region, West Iberia, Tectonics, 15, 641–659.

Ribeiro A., 2002. Soft plate and impact tectonics, Springer-Verlag, 324 p.

Reid, H.F., 1914. The Lisbon earthquake of November 1, 1755, Bull. Seism. Soc. Am., 4(2), 53–80.

Rocha, J.P., Bezzeghoud, M., Caldeira, B., Araújo, A., Borges, J.F., Vilallonga, F., & Dorbath, C.: Microseismicity in the neighbourhood of "Almodôvar fault", 6ª Assembleia Luso Espanhola de Geodesia e Geofísica, 2008. (In Portuguese)

Rocha, J.P., 2010. Tomografia sísmica da litosfera continental algarvia. Master thesis, University of Évora, 111 p.

Scheffers, A. & Kelletat, D., 2005. Tsunami relics on the coastal landscape west of Lisbon, Portugal, Science of Tsunami Hazards, 23(1), 3–16.

Sousa, M. L., A. Martins and C. S. Oliveira, 1992. Compilação de catálogos sísmicos da região Ibérica. Relatório 36/92, NDA, Laboratório Nacional de Engenharia Civil, Lisboa.

Stich, D., C.J. Ammon, & J. Morales, 2003. Moment tensor solutions for small and moderate earthquakes in the Ibero-Maghreb region. J. Geophys. Res. 108, 2148.

Terrinha, P.A.G., 1998. Structural geology and tectonic evolution of the Algarve basin, South Portugal. PhD thesis, Royal School of Mines, Imperial College. London, 423 pp.

Terrinha P., L. M. Pinheiro, J.-P. Henriet, L. Matias, Ivanov M. K., Monteiro J. H., Akhmetzhanov A., Volkonskaya A., Cunha T., Shaskin P., & Rovere M., 2003, Tsunamigenic-seismogenic structures, neotectonics, sedimentary processes and slope instability on the southwest Portuguese Margin, Mar. Geol. 195, 55-73.

Teves-Costa, P., Borges, J.F., Rio, I., Ribeiro, R. & Marreiros, C., 1999. Source parameters of old earthquakes: semi-automatic digitalization of analog records and seismic moment assessment, Nat. Hazards, 19, 205–220.

Watson D.F., 1982. Automatic Contouring of Raw Data, Computers and Geosciences, Pergamon Press Ltd., 1, 8, 97-101.

Zitellini, N. et al., 2001. Source of the 1755 Lisbon earthquake and tsunami investigated, EOS Trans. Amer. Geophys. U., 82, 285.

Zitellini N., E. Gràcia, L. Matias, P. Terrinha, M.A. Abreu, G. DeAlteriis, J.P. Henriet, J.J. Dañobeitia, D.G. Masson, T. Mulder, R. Ramella, L. Somoza, S. Diez, 2009. The quest for the Africa–Eurasia plate boundary west of the Strait of Gibraltar. Earth and Planetary Science Letters 280, 13–50.